Title: **Human posterior insula to posterior cingulate functional connectivity is related to the subjective intensity of acute pain**

Christopher J. Becker, MD, MA[a], Keith M. Vogt, MD, PhD[b], James W. Ibinson, MD, PhD[c]

[a] Department of Neurology, University of Michigan, Ann Arbor, MI 48109

      email: cbec@med.umich.edu

[b] Department of Anesthesiology, University of Pittsburgh, Pittsburgh, PA 15213

      email: vogtkm@umpc.edu

[c] Department of Anesthesiology, University of Pittsburgh, Pittsburgh, PA 15213

      email: ibinsonjw@umpc.edu

Corresponding Author:

James W. Ibinson, MD, PhD

3459 Fifth Ave

Suite 469; Montefiore Hospital

Pittsburgh, PA 15213

412-647-6465 (phone)

Ibinsonjw@upmc.edu

ORCID: 0000-0002-5525-5225

Abstract

Background: Several studies have shown that, in the context of chronic pain, alterations in functional connectivity between the insula and default mode network (DMN) are correlated with pain intensity. However, it is unknown whether a similar relationship between insula-to-DMN connectivity and pain intensity exists in the absence of chronic pain. Our aims were 1) to assess whether insula-to-DMN connectivity changes are correlated to the intensity of ongoing acute pain in healthy subjects, and 2) provide an initial assessment of the capacity of pIns-to-PCC connectivity to differentiate between painful and non-painful states. 3T BOLD functional imaging data were obtained from 13 healthy human subjects in three conditions: rest, non-painful tactile stimulation, and capsaicin-induced pain.

Results: Posterior insula to posterior cingulate (pIns-to-PCC) connectivity was significantly correlated with pain intensity. Additionally, we found that discrimination between painful and non-painful states could be achieved based on pIns-to-PCC connectivity.

Conclusions: Functional connectivity alterations in healthy subjects experiencing acute ongoing pain are similar to those observed in chronic pain patients, and can be used to classify pain state. This suggests that the inclusion of the pIns and PCC regions in future fcMRI-based methods to detect ongoing pain is warranted.

2

Background

Functional connectivity MRI is a technique that relies on correlations in spontaneous, low frequency (<0.1 Hz) fluctuations of the blood-oxygen level dependent (BOLD) signal. These correlations reveal coherent networks of anatomically distinct, yet functionally connected brain regions, even in the absence of experimental stimuli (Biswal et al. 1995; Fox et al. 2005). One prominent example is the default mode network (DMN), which typically consists of brain structures that show greater connectivity at rest than during task performance, and is thought to be involved in self-referential thinking and retrieval of autobiographical memory (Buckner et al. 2008; Mak et al. 2016). Both acute and chronic pain are associated with alterations in connectivity involving the DMN (Baliki et al. 2014; Mantini et al. 2009), particularly the posterior cingulate cortex (PCC), which is a central hub within the DMN (Fransson and Marrelec 2008; Leech et al. 2012).

The insula is an important area for pain processing (Apkarian et al. 2005; Garcia-Larrea 2012; Segerdahl et al. 2015). Connectivity between the insula and DMN has been shown to be characteristically altered by chronic pain (Baliki et al. 2014). Specifically, in chronic pain patients, insula-to-DMN connectivity is increased in proportion to pain intensity (Baliki et al. 2014; Napadow et al. 2010), with pain-exacerbating maneuvers further increasing insula-to-DMN connectivity (Loggia et al. 2013), and pain relief leading to decreased connectivity (Ceko et al. 2015; Napadow et al. 2012). Taken together, these findings suggest that, in the context of chronic pain, alterations in insula-to-DMN connectivity track changes in pain intensity.

In the absence of chronic pain, however, it is unclear whether such a relationship exists. We previously demonstrated that posterior insula (pIns) to PCC connectivity is selectively altered (as opposed to the anterior insula) in response to acute pain created by electrical nerve stimulation in healthy subjects (Vogt et al. 2016). It is unknown, however, whether the magnitude of connectivity change is related to the intensity in acute pain. Furthermore, it is unclear whether previously observed pIns-to-PCC connectivity changes are pain-modality specific, or would be seen in response to any salient stimulus.

The primary aim of this study was to investigate whether posterior insula-to-DMN connectivity is altered in proportion to pain intensity in healthy subjects when using capsaicin as source of acute pain. To do this, we compared whole-brain functional connectivity during ongoing acute pain to connectivity at rest, as well as during a salient non-painful control condition. We focused specifically on pIns-to-PCC connectivity. Our hypotheses were 1) pIns-to-PCC connectivity would be altered in proportion to pain intensity, and 2) this connectivity would not be altered by salient, but non-painful sensory stimulation. A secondary aim was to provide an initial assessment of the capacity of pIns-to-PCC connectivity to discriminate between painful and non-painful states.

Methods

Subjects

Institutional Review Board approval was obtained from the University of Pittsburgh, and informed consent was obtained from each subject. A total of 13 right-handed healthy adults (6 male) between the ages of 24-35 participated. Exclusion criteria included diagnosis of a neurologic disease, use of prescription medications or illicit drugs, pregnancy, and any contraindication to MRI. Due to the pilot nature of this study, subjects were enrolled in two cohorts. The first six subjects were in Cohort 1, the next seven in Cohort 2. All data were combined across cohorts for analysis.

Experimental Conditions

Two scans were obtained from each subject in Cohort 1. The first was a rest scan, in which subjects were instructed to not think of anything in particular and to keep their eyes open. They were not instructed to maintain focus on any particular object (i.e., no fixation cross was projected into the scanner). The second scan occurred after the application of a capsaicin-soaked 1x1 cm gauze pad to the left volar forearm. The capsaicin solution was diluted to a concentration of 0.004 Molar in 70% ethanol, and the pad was covered with waterproof adhesive film. Scans were obtained an average of 25 minutes after the application of capsaicin (range 22-28 minutes).

In Cohort 2, four scans were obtained from each subject. The first was a rest scan, identical to Cohort 1. The second was a touch scan, which was obtained as a researcher continuously moved a gauze pad around the left volar forearm of each

subject. Velocity, direction, and pressure were continuously varied to maximize the salience of this stimulus. Subjects were instructed to attend to this tactile stimulus, and were told that they would be asked questions about it after the procedure. After application of capsaicin, which was done in an identical manner to Cohort 1, the third and fourth scans occurred. An initial scan was obtained immediately after the application of capsaicin, and a final scan was obtained once pain ratings had reached at least 5/10. This occurred an average of 18 minutes after application of capsaicin (range 14-23 minutes).

The sensation elicited by the topical application of capsaicin typically begins with a period of "tingling", followed by increasingly intense pain, the timing of which varies from subject to subject. Thus, the initial set of capsaicin scans from Cohort 2 were expected to capture mostly the tingling aspect, although some would likely experience mild pain, whereas the second set was expected to capture moderate to severe pain in all subjects. Thus, scans were assigned to one of three conditions for analysis: *Rest*, *Pain*, and *Tactile Sensation*. *Rest* included all of the resting scans without stimulation. *Pain* included all of the capsaicin scans that were associated with a pain rating of 3/10 or greater. *Tactile Sensation* included all of the touch scans, as well as any capsaicin scans that were associated with a pain rating of 2/10 or lower, as this sensation was most commonly described as tingling instead of pain.

Data Acquisition

Subjective pain ratings were obtained at the end of each capsaicin scan. Subjects responded by verbally rating the intensity of their pain on a scale from 0 to 10, with 0 representing no pain and 10 representing the worst pain imaginable. In

6

the rest and touch conditions, subjects verbally confirmed that they did not experience pain during the scan. Salience ratings for the touch and capsaicin stimuli were also obtained after completion of the procedure by the subjects in Cohort 2. They responded on a scale from 0 to 10, with 0 being "not prominent in your thoughts at all" and 10 being "something that you could not take you mind off".

The functional scans for Cohort 1 were each six minutes in duration. For Cohort 2, each functional scan lasted eight minutes. For all subjects in both cohorts, a single high-resolution structural image was obtained. Images for Cohort 1 were collected with a 3.0-T Siemens Trio scanner (Siemens Medical Solutions USA, Inc, Malvern, PA). High-resolution structural images were collected for each participant to facilitate the creation of group maps using a T1-weighted scanning technique (MPRAGE sequence, TR/TE/Flip = 1.6 s/3.18 ms/8°; field of view = 256 cm x 240 cm; slice thickness = contiguous 1.2 mm; in-plane resolution = 1.0 mm). Functional images were collected using a BOLD sensitive single-shot gradient echo, T2*-weighted sequence (TR/TE/ Flip = 2 s/30 ms/90°; 64 x 64 matrix; slice thickness = 3 mm, in-plane resolution = 3.125 x 3.125 mm). Twenty-eight axial slices with no gaps were acquired in an interleaved fashion.

Images for Cohort 2 were collected with a Siemens Allegra 3T MRI Head-Scanner. An MPRAGE sequence (TR/TE/Flip = 1.54 s/3.04 ms/8°; field of view = 256 mm x 256 mm; slice thickness = contiguous 1 mm; in-plane resolution = 1 mm; matrix = 256 x 256) was again used for high-resolution scanning. Functional imaging consisted of 38 axial slices collected with BOLD weighted single-shot

gradient echo parameters (TR/TE/ Flip = 2 s/25 ms/70°; 64 x 64 matrix; slice

thickness = 3.2 mm, in-plane resolution = 3.125 x 3.125 mm).

Data Analysis

All functional images were preprocessed within MATLAB (Mathworks Inc.,

Natick, MA, USA) using the Functional Connectivity Toolbox, version 15.e (Whitfield-

Gabrieli and Nieto-Castanon 2012). Preprocessing included realignment, slice

timing correction, segmentation, normalization, and spatial smoothing using a

Gaussian kernel of full width at half maximum of 6 mm. Each participant's functional

images were registered to their high-resolution T1-weighted structural image, and

to the MNI152 standard space template. The preprocessed data were band-pass

filtered (0.009 < f < 0.08 Hz), and motion artifacts were removed by linear

regression of six motion parameters obtained by rigid body correction of motion of

the head. Grey matter, white matter, and CSF signals were included as regressors of

no interest, as this has been shown to improve specificity for connectivity maps of

pain (Ibinson et al. 2015).

BOLD signal time courses were extracted from a pre-defined ROI in the right

posterior insula, contralateral to the touch and capsaicin stimuli. This ROI was

defined as a sphere with a radius of 6 mm centered around MNI coordinates 38, -4,

10, as identified in a previous study of acute electrical nerve stimulation pain

(Ibinson and Vogt 2013). The signal was averaged across the voxels within this ROI

for each subject, and the resulting time courses were used as explanatory variables

in a seed-based analysis. Using procedures established by Fox et al. (Fox et al. 2005),

correlation maps were generated by computing the correlation coefficient between

8

the seed time courses and the time courses from each of the voxels in the brain. Additionally, ROI-to-ROI correlation values were obtained by computing correlation coefficients between the pIns seed region and a ROI corresponding to Broadmann Area 31 (BA31), which includes the PCC.

To assess whether pIns-to-PCC connectivity was altered in relation to perceived pain intensity, a Spearman's rank order correlation coefficient was computed. This non-parametric test was used because it is robust to outliers. Next, a Kruskal-Wallis test one way ANOVA by ranks was conducted to compare average pIns-to-PCC connectivity values across conditions (i.e., *Rest*, *Pain*, and *Tactile Sensation*). Lastly, a receiver operating characteristic (ROC) curve was generated to assess the discrimination performance of pIns-to-PCC connectivity across multiple thresholds. Group average connectivity maps for *Rest*, *Tactile Sensation*, and *Pain* were generated using a second level mixed-effects analysis in Conn Toolbox. Significant clusters are shown with FDR-corrected threshold of $p < 0.05$. All images are displayed in neurologic convention, with warm colors representing positive correlations, and cool colors representing anti-correlations.

Results

Psychophysical results

No subject in either cohort reported experiencing pain during the rest or touch scans; accordingly, these were assigned a pain rating of 0. In Cohort 1, the median (range) subjective pain ratings for the capsaicin scans was 4.5 (0 to 8). One subject from Cohort 1 did not feel pain with the capsaicin stimulus, and reported

pain ratings of 0 throughout. This subject's capsaicin scan was therefore grouped with the *Tactile Sensation* scans. In Cohort 2, the median (range) subjective pain ratings for the first and second capsaicin scans were 3 (1 to 3) and 7 (4 to 7), respectively. Subjective ratings of the salience of the touch and capsaicin stimuli were collected from subjects in Cohort 2. The median (range) of the salience ratings was 6.25 (3 to 8) for the touch stimuli, and 6.5 (4 to 9) for the capsaicin stimuli. A Wilcoxon rank-sum test revealed no significant difference in salience ratings, $Z = 0.162$, $p = 0.871$.

fcMRI results

A total of 40 scans were obtained (two scans each from 6 subjects in Cohort 1, and four scans each from 7 subjects in Cohort 2). These were divided into 3 categories as described in section 4.2, resulting in a total of 13 *Rest* scans, 11 *Tactile Stimulation* scans, and 16 *Pain* scans. Group average functional connectivity maps using the pIns as the seed region for each category are shown in Figure 1. Panel A shows all regions with significant connectivity to the pIns in the *Rest* scans, Panel B shows the same for the *Tactile Sensation* scans, and Panel C for the *Pain* scans. The *Rest* map is notable for significant pIns anti-correlations to the PCC/precuneus. The *Pain* map is notable for the lack of the pIns-PCC anti-correlations seen in *Rest*, and for positive connectivity between the pIns and the anterior cingulate cortex (ACC). Other areas of connectivity to the pIns (with the magnitude of correlation indicated by T-max values) are provided in Tables 1-3. Table 1 contains significant connectivity clusters for the *Rest* scans, Table 2 for the *Tactile Sensation* scans, and Table 3 for the *Pain* scans.

10

Association between pIns-to-PCC connectivity and pain

To assess the relationship between pIns-to-PCC connectivity and subjective pain intensity, a Spearman's rank order correlation coefficient was computed. This was found to be significant, with increased pain ratings being associated with increased pIns-to-PCC connectivity, r_s (38) = 0.34, p = 0.032. A scatter plot showing the relationship between connectivity values and subjective pain ratings from all capsaicin scans is shown in Figure 2.

The mean (standard deviation) of pIns-to-PCC connectivity values across conditions were as follows: *Rest* -0.18 (0.15), *Tactile Sensation* -0.10 (0.11), and *Pain* -0.04 (0.14). Note that negative connectivity frequently occurs as a result of global signal regression, and does not necessarily represent "deactivation". A graphical representation of these values can be found in Figure 3. A Kruskal-Wallis test revealed significant differences in connectivity across conditions, H(2) = 9.36, p = 0.0093. Post hoc comparisons using t-test, with Bonferroni correction, revealed significant differences in connectivity between the *Rest* and *Pain* scans, p = 0.012. Because of the graded pattern of connectivity strength, the differences between the *Rest* and *Tactile Sensation* scans and between the *Tactile Sensation* and *Pain* scans were not statistically significant.

Lastly, to assess the overall capacity of pIns-to-PCC connectivity to differentiate *Pain* scans from *Rest* and *Tactile Sensation* scans, a receiver operating characteristic (ROC) curve was generated. The area under the curve was found to be significant at 0.75 (95% CI = 0.59 – 0.91; p = .008). This is shown in Figure 4.

Discussion

Several studies have identified a correlation between insula-to-DMN connectivity and pain intensity in chronic pain patients (Baliki et al. 2014; Loggia et al. 2013; Napadow et al. 2010). We now report a similar relationship between insula-to-DMN connectivity and pain intensity in healthy subjects who are experiencing ongoing acute pain. Additionally, in chronic pain patients, maneuvers that exacerbate chronic pain further alter insula-to-DMN connectivity (Loggia et al. 2013), while pain relief is associated with shifts toward baseline connectivity (Ceko et al. 2015; Napadow et al. 2012). Taken together, these findings point to a relationship between insula-to-DMN connectivity and the magnitude of ongoing pain in both healthy subjects and chronic pain patients. This suggests that the observed connectivity changes in chronic pain patients may be related to ongoing pain rather than more permanent underlying alterations.

Previous studies have identified insula-to-DMN connectivity changes in response to acute pain (Ibinson et al. 2015; Zhang et al. 2014). However, these studies did not attempt to quantify the relationship between pain intensity and changes in connectivity, as was done here. Furthermore, these studies did not include a non-painful control condition. This makes interpretation difficult, as it could be argued that their results simply reflect differences in salience across conditions, rather than pain specific responses. In support of this possible interpretation, there is evidence that patterns of neural activity seen in response to pain largely overlap with patterns seen in response to other salient stimuli (Iannetti and Mouraux 2010; Legrain et al. 2011; Liberati et al. 2016). We included a salient

12

non-painful control condition in an attempt to address this issue, hypothesizing that pIns-to-PCC connectivity would not be altered by salient non-painful stimulation. This was supported by the observation that the rest and tactile stimulation conditions did not significantly differ in terms of pIns-to-PCC connectivity, whereas there was a significant difference between the rest and pain conditions.

Yet it could still be argued that our results simply reflect the greater salience of a painful stimulus relative to a touch stimulus, since connectivity also did not significantly differ between the *Tactile Sensation* and *Pain* conditions and the lack of a difference between *Rest* and *Tactile Sensation* could be attributed to low power. While this cannot be definitively ruled out, the subjective salience ratings we obtained for the touch and capsaicin stimuli did not differ, making an explanation based purely on stimulus salience less likely.

Our secondary aim was to assess the strength of pIns-to-PCC connectivity as a classifier of pain state. This was accomplished through a ROC curve analysis, which showed significant classification accuracy for pIns-to-PCC connectivity in discriminating pain states from non-pain states (i.e., *Rest* and *Tactile Sensation*). Several groups have previously demonstrated the utility of fMRI in detecting pain, though with important limitations (Brown et al. 2011; Marquand et al. 2010). Perhaps the best example comes from Wager et al. (Wager et al. 2013), who used task-based fMRI and machine learning to develop a model capable of accurately differentiating pain from warmth and other aversive events. While this represents a significant achievement, the potential applications of this approach are limited by the reliance on a block-design paradigm, which requires the repeated presentation

of an experimental stimulus. In contrast, a functional connectivity-based approach would not necessarily require an experimental stimulus. Such a technique would be better suited to measure ongoing pain, as would be seen in clinical populations. The present findings suggest that such an fcMRI-based approach may be possible.

The posterior insula was the focus of the present study. There are several lines of evidence to suggest that this region plays a key role in pain processing. First, anatomical studies in primate models have revealed projections from pain sensitive thalamic nuclei to the posterior insula (Burton and Jones 1976; Friedman and Murray 1986; Mufson and Mesulam 1984). In fact, the posterior insula has been shown to receive more spinothalamic input than any other cortical area (Dum et al. 2009). Second, consistent with these anatomical connections, the insula is the region most commonly activated in response to pain across imaging studies (Apkarian et al. 2005). Furthermore, Segerdahl et al. (Segerdahl et al. 2015) found that blood flow in the pIns was correlated with induced fluctuations in pain intensity over time. Third, lesion studies show that damage to the posterior insula leads to increased pain thresholds (Birklein et al. 2005; Bowsher et al. 2004; Greenspan and Winfield 1992; Kim 2007; Schmahmann and Leifer 1992), while lesions to the anterior insula do not (Greenspan et al. 1999). Posterior insular lesions are also implicated pain asymbolia, a condition where patients demonstrate no primary sensory defects, yet fail to show typical emotional and withdrawal responses to painful stimuli (Berthier et al. 1988). Finally, electrical stimulation of the posterior insula and adjacent parietal operculum can evoke painful sensations (Isnard et al. 2004; Mazzola et al. 2009; Ostrowsky et al. 2002). While only a minority of stimuli applied to this region

cause pain, no other cortical region has been shown to give rise to pain when electrically stimulated (Mazzola et al. 2012). A case has also been reported of a patient with purely painful seizures who was found to have an epileptogenic focus in the posterior insula, further suggesting that the experience of pain can be generated by neural activity originating in this region (Isnard et al. 2011). In sum, the posterior insula shares anatomical connections with ascending pain pathways, shows blood flow that is correlated with perceived pain intensity, leads to decreased pain sensitivity when damaged, and gives rise to pain when stimulated. While it should be noted that this region is involved in a wide range of functions (Nieuwenhuys 2012), these findings nonetheless suggest an important role for the posterior insula that is specific to pain processing. Thus, it is unsurprising that a measure based on connectivity of this region would be useful in the detection of pain. In fact, the pIns was among the regions assigned the highest predictive weight in the Wager et al. (2013) pain detection model.

Similarly, the DMN seems to be characteristically affected by pain. Baliki et al. (Baliki et al. 2014) examined the effects of several chronic pain conditions on multiple resting state networks (RSNs), and found the DMN to be the only RSN consistently altered across chronic pain conditions. The authors also noted corresponding changes in insula-to-DMN connectivity in association with chronic pain. Similar alterations have been reported in a number of chronic pain conditions including fibromyalgia (Napadow et al. 2010), chronic back pain (Tagliazucchi et al. 2010), complex regional pain syndrome (Baliki et al. 2014), diabetic neuropathic pain (Cauda et al. 2009), and osteoarthritis (Baliki et al. 2014). Moreover, Ichesco et

15

al. (Ichesco et al. 2014) specifically found altered pIns-to-PCC connectivity in fibromyalgia patients compared to controls.

As noted above, the current study is limited by the use of a relatively small sample and the reliance on a single pain stimulus. It is worth noting that our findings are consistent with results obtained using an electrical pain stimulus in healthy subjects (Ibinson et al. 2015), and, as noted above, are broadly consistent with studies involving chronic pain patients. Additionally, we collected data using different parameters on two separate scanners, but still found that the relationship between connectivity and pain intensity persisted. This tempers concerns about the methodology and adds to the robustness of these findings.

Conclusions

In summary, we have demonstrated that ongoing pain in healthy subjects causes alterations in posterior insula-to-DMN connectivity in proportion to perceived pain intensity. These findings are not explained entirely by salience. Our results share similarities with previous reports of connectivity changes in chronic pain patients, yet we expand on this prior work by demonstrating corresponding alterations in response to acute pain in healthy subjects. Furthermore, pain state can be classified based on pIns-to-PCC connectivity.. These findings suggest that, with further development, fcMRI measures based in part on pIns-to-PCC connectivity may hold promise as a noninvasive biomarker for pain.

Declarations

<u>Ethics approval and consent to participate</u>: Institutional Review Board approval was obtained from the University of Pittsburgh, and informed consent was obtained from each subject. All procedures performed in studies involving human participants were in accordance with the ethical standards of the institutional and/or national research committee and with the 1964 Helsinki declaration and its later amendments or comparable ethical standards.

<u>Consent for publication</u>: not applicable

<u>Availability of data and material</u>: The datasets used and/or analyzed during the current study are available from the corresponding author on reasonable request.

<u>Competing interests</u>: The authors declare no competing financial interests

<u>Authors' contributions</u>: CB, KV, and JI all made substantial contributions to conception, design, acquisition of data, analysis and interpretation of data, and drafting and revising the manuscript.

References

Apkarian AV, Bushnell MC, Treede RD, Zubieta JK (2005) Human brain mechanisms of pain perception and regulation in health and disease Eur J Pain 9:463-484 doi:10.1016/j.ejpain.2004.11.001

Baliki MN, Mansour AR, Baria AT, Apkarian AV (2014) Functional reorganization of the default mode network across chronic pain conditions PLoS One 9:e106133 doi:10.1371/journal.pone.0106133

Berthier M, Starkstein S, Leiguarda R (1988) Asymbolia for pain- a sensory-limbic disconnection syndrome Ann Neurol 24:41-49

Birklein F, Rolke R, Muller-Forell W (2005) Isolated insular infarction eliminates contralateral cold, cold pain, and pinprick perception Neurology 65:1381 doi:10.1212/01.wnl.0000181351.82772.b3

Biswal B, Yetkin FZ, Haughton VM, Hyde JS (1995) Functional connectivity in the motor cortex of resting human brain using echo-planar MRI Magn Reson Med 34:537-541

Bowsher D, Brooks J, Enevoldson P (2004) Central representation of somatic sensations in the parietal operculum (SII) and insula Eur Neurol 52:211-225 doi:10.1159/000082038

Brown JE, Chatterjee N, Younger J, Mackey S (2011) Towards a physiology-based measure of pain: patterns of human brain activity distinguish painful from non-painful thermal stimulation PLoS One 6:e24124 doi:10.1371/journal.pone.0024124

Buckner RL, Andrews-Hanna JR, Schacter DL (2008) The brain's default network:

    anatomy, function, and relevance to disease Ann N Y Acad Sci 1124:1-38

    doi:10.1196/annals.1440.011

Burton H, Jones EG (1976) The Posterior Thalamic Region and Its Cortical Projection

    in New World and Old World Monkeys Journal of Comparative Neurology

    168:249-284

Cauda F, Sacco K, Duca S, Cocito D, D'Agata F, Geminiani GC, Canavero S (2009)

    Altered resting state in diabetic neuropathic pain PLoS One 4:e4542

    doi:10.1371/journal.pone.0004542

Ceko M, Shir Y, Ouellet JA, Ware MA, Stone LS, Seminowicz DA (2015) Partial

    recovery of abnormal insula and dorsolateral prefrontal connectivity to

    cognitive networks in chronic low back pain after treatment Hum Brain

    Mapp 36:2075-2092 doi:10.1002/hbm.22757

Dum RP, Levinthal DJ, Strick PL (2009) The spinothalamic system targets motor and

    sensory areas in the cerebral cortex of monkeys J Neurosci 29:14223-14235

    doi:10.1523/JNEUROSCI.3398-09.2009

Fox MD, Snyder AZ, Vincent JL, Corbetta M, Van Essen DC, Raichle ME (2005) The

    human brain is intrinsically organized into dynamic, anticorrelated

    functional networks Proc Natl Acad Sci U S A 102:9673-9678

    doi:10.1073/pnas.0504136102

Fransson P, Marrelec G (2008) The precuneus/posterior cingulate cortex plays a

    pivotal role in the default mode network: Evidence from a partial correlation

network analysis Neuroimage 42:1178-1184
doi:10.1016/j.neuroimage.2008.05.059

Friedman DP, Murray EA (1986) Thalamic connectivity of the second
somatosensory area and neighboring somatosensory fields of the lateral
sulcus of the macaque Journal of Comparative Neurology 252:348-373

Garcia-Larrea L (2012) The posterior insular-opercular region and the search of a
primary cortex for pain Neurophysiol Clin 42:299-313
doi:10.1016/j.neucli.2012.06.001

Greenspan JD, Lee RR, Lenz FA (1999) Pain sensitivity alterations as a function of
lesion location in the parasylvian cortex Pain 81:273-282

Greenspan JD, Winfield JA (1992) Reversible pain and tactile deficits associated with
a cerebral tumor compressing the posterior insula and parietal operculum
Pain 50:29-39

Iannetti GD, Mouraux A (2010) From the neuromatrix to the pain matrix (and back)
Exp Brain Res 205:1-12 doi:10.1007/s00221-010-2340-1

Ibinson JW, Vogt KM (2013) Pain does not follow the boxcar model: temporal
dynamics of the BOLD fMRI signal during constant current painful electric
nerve stimulation J Pain 14:1611-1619 doi:10.1016/j.jpain.2013.08.004

Ibinson JW, Vogt KM, Taylor KB, Dua SB, Becker CJ, Loggia M, Wasan AD (2015)
Optimizing and Interpreting Insular Functional Connectivity Maps Obtained
During Acute Experimental Pain: The Effects of Global Signal and Task
Paradigm Regression Brain connectivity 5:649-657
doi:10.1089/brain.2015.0354

Ichesco E et al. (2014) Altered resting state connectivity of the insular cortex in
individuals with fibromyalgia J Pain 15:815-826 e811
doi:10.1016/j.jpain.2014.04.007

Isnard J, Guenot M, Sindou M, Mauguiere F (2004) Clinical Manifestations of Insular
Lobe Seizures-A Stereo-electroencephalographic Study Epilepsia 45:1079-
1090

Isnard J, Magnin M, Jung J, Mauguiere F, Garcia-Larrea L (2011) Does the insula tell
our brain that we are in pain? Pain 152:946-951
doi:10.1016/j.pain.2010.12.025

Kim JS (2007) Patterns of sensory abnormality in cortical stroke: evidence for a
dichotomized sensory system Neurology 68:174-180
doi:10.1212/01.wnl.0000251298.12763.9b

Leech R, Braga R, Sharp DJ (2012) Echoes of the Brain within the Posterior Cingulate
Cortex J Neurosci 32:215-222

Legrain V, Iannetti GD, Plaghki L, Mouraux A (2011) The pain matrix reloaded: a
salience detection system for the body Prog Neurobiol 93:111-124
doi:10.1016/j.pneurobio.2010.10.005

Liberati G, Klocker A, Safronova MM, Ferrao Santos S, Ribeiro Vaz JG, Raftopoulos C,
Mouraux A (2016) Nociceptive Local Field Potentials Recorded from the
Human Insula Are Not Specific for Nociception PLoS Biol 14:e1002345
doi:10.1371/journal.pbio.1002345

Loggia ML et al. (2013) Default mode network connectivity encodes clinical pain: an
arterial spin labeling study Pain 154:24-33 doi:10.1016/j.pain.2012.07.029

Mak LE, Minuzzi L, MacQueen G, Hall G, Kennedy S, Milev R (2016) The Default Mode

Network in Healthy Individuals: A Systematic Review and Meta-Analysis

Brain connectivity doi:10.1089/brain.2016.0438

Mantini D, Caulo M, Ferretti A, Romani GL, Tartaro A (2009) Noxious somatosensory

stimulation affects the default mode of brain function- evidence from

functional MR imaging Radiology 253:797-804

doi:10.1148/radiol.2533090602/-/DC1

Marquand A, Howard M, Brammer M, Chu C, Coen S, Mourao-Miranda J (2010)

Quantitative prediction of subjective pain intensity from whole-brain fMRI

data using Gaussian processes Neuroimage 49:2178-2189

doi:10.1016/j.neuroimage.2009.10.072

Mazzola L, Isnard J, Peyron R, Guenot M, Mauguiere F (2009) Somatotopic

organization of pain responses to direct electrical stimulation of the human

insular cortex Pain 146:99-104 doi:10.1016/j.pain.2009.07.014

Mazzola L, Isnard J, Peyron R, Mauguiere F (2012) Stimulation of the human cortex

and the experience of pain: Wilder Penfield's observations revisited Brain

135:631-640 doi:10.1093/brain/awr265

Mufson EJ, Mesulam MM (1984) Thalamic connections of the insula in the rhesus

monkey and comments on the paralimbic connectivity of the medial pulvinar

nucleus J Comp Neurol 227:109-120 doi:10.1002/cne.902270112

Napadow V, Kim J, Clauw DJ, Harris RE (2012) Decreased intrinsic brain

connectivity is associated with reduced clinical pain in fibromyalgia Arthritis

Rheum 64:2398-2403 doi:10.1002/art.34412

Napadow V, LaCount L, Park K, As-Sanie S, Clauw DJ, Harris RE (2010) Intrinsic

brain connectivity in fibromyalgia is associated with chronic pain intensity

Arthritis Rheum 62:2545-2555 doi:10.1002/art.27497

Nieuwenhuys R (2012) The insular cortex: a review Prog Brain Res 195:123-163

doi:10.1016/B978-0-444-53860-4.00007-6

Ostrowsky K, Magnin M, Ryvlin P, Isnard J, Guenot M, Mauguiere F (2002)

Representation of pain and somatic sensation in the human Insula: A study of

responses to direct electrical cortical stimulation Cereb Cortex 12:376-385

Schmahmann JD, Leifer D (1992) Parietal Pseudothalamic Pain Syndrome Clinical

Features and Anatomic Correlates Arch Neurol 49:1032-1037

Segerdahl AR, Mezue M, Okell TW, Farrar JT, Tracey I (2015) The dorsal posterior

insula subserves a fundamental role in human pain Nat Neurosci 18:499-500

doi:10.1038/nn.3969

Tagliazucchi E, Balenzuela P, Fraiman D, Chialvo DR (2010) Brain resting state is

disrupted in chronic back pain patients Neurosci Lett 485:26-31

doi:10.1016/j.neulet.2010.08.053

Vogt KM, Becker CJ, Wasan AD, Ibinson JW (2016) Human Posterior Insula

Functional Connectivity Differs Between Electrical Pain and the Resting State

Brain Connect 6:786-794 doi:10.1089/brain.2016.0436

Wager TD, Atlas LY, Lindquist MA, Roy M, Woo CW, Kross E (2013) An fMRI-based

neurologic signature of physical pain N Engl J Med 368:1388-1397

doi:10.1056/NEJMoa1204471

Whitfield-Gabrieli S, Nieto-Castanon A (2012) Conn: a functional connectivity

toolbox for correlated and anticorrelated brain networks Brain Connect

2:125-141 doi:10.1089/brain.2012.0073

Zhang S, Wu W, Huang G, Liu Z, Guo S, Yang J, Wang K (2014) Resting-state

connectivity in the default mode network and insula during experimental low

back pain Neural Regen Res 9:135-142 doi:10.4103/1673-5374.125341

Figure Captions

Figure 1. Group average connectivity maps. Maps reflect connectivity to the pIns seed region for *Rest* (panel A), *Tactile Sensation* (panel B), and *Pain* (panel C). Significant correlations are shown in red, and anti-correlations are shown in blue (FDR-corrected p < 0.05). The *Rest* map demonstrates resting-state anti-correlations between the pIns and the PCC/precuneus. The *Pain* map is notable for the absence of resting state pIns-to-PCC anti-correlations, as well as positive connectivity to the anterior cingulate cortex (ACC).

Figure 2. Relationship between connectivity and pain intensity. Scatter plot with linear trendline illustrating the positive correlation between subjective pain ratings and pIns-to-PCC connectivity for all capsaicin scans.

Figure 3. Mean pIns-to-PCC connectivity and standard error by condition. Connectivity was most negative for the *Rest* scans, and least negative for the *Pain* scans. The means were found to significantly differ across conditions, $F(2,37) = 4.75$, $p = 0.015$. Post hoc analyses revealed a significant difference between *Rest* and *Pain*, and not between *Rest* and *Tactile Sensation*; *$p < 0.05$.

Figure 4. ROC curve for pIns-to-PCC connectivity in classifying pain state. This receiver operating characteristic (ROC) curve shows the classification performance of pIns-to-PCC connectivity in detecting pain across various discrimination thresholds. Area under the curve = 0.75, $p < 0.01$.

Tables

Table 1. Regions with significant connectivity to the pIns in the Rest condition

Brain Region	Size	T	x, y, z
Left Insula	743	17.2	-44, 0, 0
Right Insula	401	13.07	40, 0, 10
Precuneus	230	-17.04	-8, -58, 36
Left postcentral gyrus	135	10.37	-62, 2, 28
Right postcentral gyrus	105	14.34	48, -24, 44
Right precentral gyrus	74	10.58	62, 10, 8
Right angular gyrus	66	-17.16	54, -54, 36
Right postcentral gyrus	59	11.05	56, -14, 26
Right frontal pole	54	-19.44	12, 66, 18
Right putamen	52	14.42	-18, 2, 4
Precuneus	49	-11.06	-2, -44, 44
Right supplementary motor cortex	46	11.15	-2, 6, 54
Right frontal orbital cortex	36	-14.56	20, 14, -18
Right frontal pole	29	-26.21	38, 50, -18

Cluster size, max T, and MNI coordinates for regions with significant connectivity to the pIns in the Rest condition. Cluster-size threshold p-FDR < 0.001, height threshold p < 0.001.

Table 2. Regions with significant connectivity to the pIns in the Tactile Sensation condition

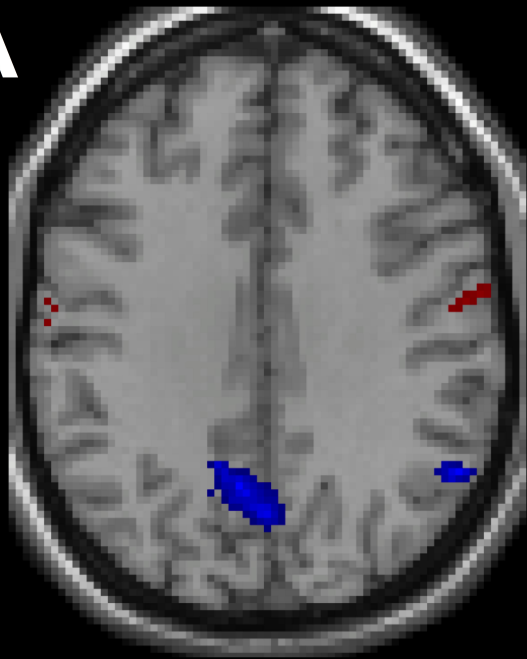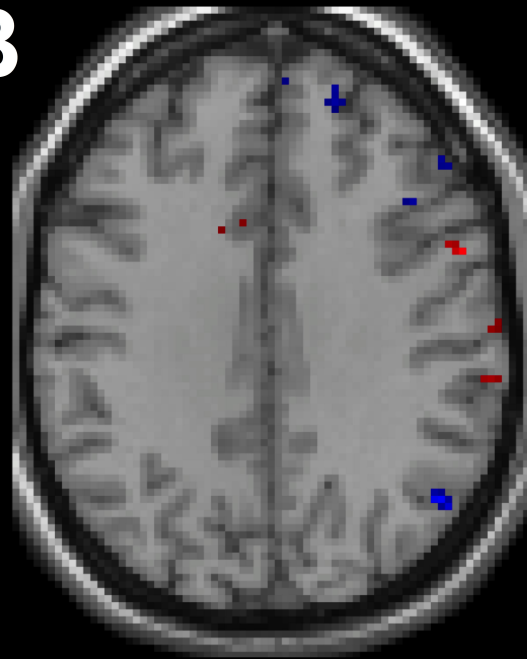| Brain Region	Size	T	x, y, z
Right central opercular cortex	1959	14.54	44, -4, 4
Left central opercular cortex	1523	14.22	-48, -32, 20
Right supplementary motor cortex	338	11.59	4, -10, 64
Left middle frontal gyrus	290	17.38	-44, 26, 50
Right middle frontal gyrus	243	-17.49	40, 16, 48
Right frontal pole	155	-14.74	20, 46, 34
Left lateral occipital cortex	82	-7.89	-46, -68, 44
Right middle temporal gyrus	69	-10.59	64, -44, -16
Right superior frontal gyrus	68	-13.35	24, 28, 64
Anterior cingulate gyrus	61	9.73	-10, 2, 40
Left superior frontal gyrus	60	-17.25	-22, 32, 56
Right lateral occipital cortex	58	-14.71	40, -66, 46
Right superior frontal gyrus	57	-11.82	-2, 42, 42
Right precentral gyrus	50	8.64	54, -10, 50
Lateral occipital cortex	49	-8.02	48, -62, 32
Right frontal pole	47	-8.53	22, 36, 54
Right precentral gyrus	40	9.73	58, -2, 42
Right putamen	40	9.28	24, 16, -12
Left temporal pole	38	11	-32, 6, -18

Cluster size, max T, and MNI coordinates for regions with significant connectivity to the pIns in the Tactile Sensation condition. Cluster-size threshold p-FDR < 0.001, height threshold p < 0.001.

Table 3. Regions with significant connectivity to the pIns in the Pain condition

Brain Region	Size	T	x, y, z
Right Insula	4598	8.21	66, -16, 34
Left Insula	1988	7.33	-44, -6, -2
Anterior cingulate gyrus	1669	8.44	2, -10, 62
Postcentral gyrus	539	8.48	14, -34, 78
Precuneus	330	-7.04	6, -66, 48
Lateral occipital cortex	307	-7.29	30, -74, 48
Right frontal pole	202	-6.13	36, 60, 0
Left occipital pole	188	-6.76	-4, -98, -6
Right frontal pole	111	-9.25	14, 66, 14

Cluster size, max T, and MNI coordinates for regions with significant connectivity to the pIns in the Pain condition. Cluster-size threshold p-FDR < 0.001, height threshold p < 0.001.